АСТРОФИЗИКА

ТОМ 67 НОЯБРЬ, 2024 ВЫПУСК 4

DOI: 10.54503/0571-7132-2024.67.4-581

MODIFIED FINCH AND SKEA STELLAR MODEL IN HIGHER DIMENSIONS

A.JANGID[1], S.DAS[2], B.S.RATANPAL[3], K.K.VENKATARATNAM[1]

Received 10 August 2024
Accepted 6 December 2024

Within the framework of higher dimensions, we enhance the model of Pandya and Thomas and assume that the system is anisotropic in the Finch and Skea ansatz. Our model explores various physical parameters in higher dimensions, including mass, energy density, radial and transverse pressures, and the anisotropy factor. We have used graphical technique to analyse the energy conditions, equilibrium conditions, and stability across different dimensions. Furthermore, the mass of a particular compact object have shown to increase with radial parameter as space-time dimensions increase. Additionally, by generating a mass-radius (M-R) plot, we demonstrate the influence of dimensional factor on the maximum mass and radius allowed by our toy model.

Keywords: *modified Finch-Skea ansatz: higher dimensions: Einstein field equations: Ricci tensor*

1. *Introduction*. The space-time geometry of Finch and Skea [1], which Duorah and Ray [2] first created, has drawn a lot of interest in the modelling of relativistic compact stars since it produces a well-behaved solution that Delgaty and Lake [3] later demonstrated to meet all the physical conditions of an actual star assuming isotropy in pressure. Nevertheless, a number of theoretical studies have demonstrated that anisotropy may arise in the high density region of compact star objects. According to Ruderman [4] and Canuto [5], the radial pressure p_r and the transverse pressure p_t do not necessarily need to be equal in the high-density regime of compact stars is reason for anisotropy. The existence of type-3A superfluid, rotation, an electromagnetic field, and other factors are among the many circumstances that Bowers and Liang [6] discussed in detail about the possibility of anisotropy in stellar interiors. As a result, several researchers have looked into the Finch-Skea model in relation to matter anisotropy like Hansraj and Maharaj [7], Ratanpal [8], Pandya [9], Maharaj et al. [10]. In the last few decades, a significant amount of study has been done to comprehend problems in astrophysics and cosmology within the context of lower as well as higher dimensions. In (2+1) dimensions, the Finch-Skea stellar model has been examined by Benergy [11], Bhar et al. [12]. Along with new physics, the results gained

in the standard four dimensions are particularly generalised in higher dimensions. Higher dimensions have their roots in the research conducted in the past by Kaluza and Klein [13,14]. In order to reconcile gravitational and electromagnetic interactions, Kaluza and Klein separately initially proposed the idea of an additional dimension in addition to the standard four dimensions. The model is basically a five-dimensional extension of Einstein's general theory of relativity, which is very relevant to both particle physics and cosmology. However, the first strategy is ineffective. After it was discovered that many intriguing ideas of particle interactions require more dimensions than four for their consistent formulation, research into higher dimensional theories was once again resurrected a few decades ago, and it was greatly expanded. The results of four-dimensional GTR needed to be generalised to a higher-dimensional setting in order to examine the consequences of adding one or more additional space-time dimensions to the theory. In order to address various issues not understood in the usual four dimensions, a number of cosmological models in higher dimensions have been discussed in the literature by Shafi [15], Wetterich [16], Wiltshire [17], Accetta et al. [18], Paul, Mukherjee [19]. Chodos and Detweiler [20,21] first obtained a higher dimensional cosmological model in this direction. It is conceivable to recover the standard four-dimensional Newtonian gravity from a five-dimensional anti-de Sitter space-time in the low energy limit, according to an intriguing description of gravity provided by Randall and Sundrum [22]. The extra dimensions are not compact.

Liddle et al. [23] examined the effects of extra dimensions on the Kaluza-Klein model's ability to explain the structure of neutron stars. As an expansion of the four dimensions, the mass to radius ratio in higher dimensions for a uniform density star is calculated, and new findings have been published in the literature by Paul [24].

With some hope for future experimental discoveries, dimensional physics is currently a busy field of study [25]. By including a dimensionless parameter D (>0) in the Finch and Skea ansatz, we have expanded the Pandya and Thomas [9] model in this work and generally assumed that the system is anisotropic. In the present work the solution of the Einstein field equation for static spherically symmetric anisotropic matter distribution in higher dimensions.

The paper has been organized as follows. In section 2, for the assumed form of the space-time metric, the relevant field equations in higher dimensions have been laid down. The modified Finch and Skea model and solution is discussed in section 3. In section 4, the exterior region which is the Schwarzschild metric is matched with the interior to obtain boundary conditions and the model parameters. In section 5, the physical viability of our model is shown in different dimensions. Finally, some concluding remarks have been made in section 6.

2. *Field equations in higher dimensions*. The Einstein field equation in higher dimensions is given by

$$\mathbf{R}_{\alpha\beta} - \frac{1}{2} g_{\alpha\beta} \mathbf{R} = 8\pi G_D T_{\alpha\beta} , \tag{1}$$

where G_D is the fundamental parameter of interest defined as the gravitational constant in higher dimensions. In higher-dimensional theories, G_D is related to the standard four-dimensional gravitational constant G by the relation $G_D = GV_{D\text{-}4}$, where $V_{D\text{-}4}$ is the volume of the extra dimensions, and D represents the total number of dimensions. The parameter G_D is inherently dependent on the dimensions. As the dimensionality D increases, the corresponding gravitational constant G_D also increases. This relationship highlights the influence of additional spatial dimensions on the gravitational interaction, making G_D a crucial aspect of the model's framework in higher-dimensional theories. $R_{\alpha\beta}$ is Ricci tensor, R is Ricci scalar, $g_{\alpha\beta}$ is metric tensor and $T_{\alpha\beta}$ is the energy momentum tensor in D dimensions.

The Einstein's field equations (EFE) describe how matter and energy influence the curvature of space-time. In vacuum regions, where no matter or energy is present, the stress-energy tensor $T_{\alpha\beta}$ is zero. The field equations then simplify to

$$\mathbf{R}_{\alpha\beta} - \frac{1}{2} g_{\alpha\beta} \mathbf{R} = 0 .$$

We write the interior space-time metric in higher dimensions of a static spherically symmetric distribution of anisotropic matter in the form

$$ds_-^2 = -e^{2\nu} dt^2 + e^{2\mu} dr^2 + r^2 d\Omega_n , \tag{2}$$

where $\nu(r)$ and $\mu(r)$ are the two unknown metric functions, $n = D - 2$ and $d\Omega_n^2 = d\theta_1^2 + \sin^2\theta_1 d\theta_1^2 + \sin^2\theta_2 \left(d\theta_3^2 + ... + \sin^2\theta_{n-1} d\theta_n^2\right)$ is a linear element on a n-dimensional unit sphere in polar coordinates parameterized by the angles $\theta_1, \theta_2, ..., \theta_n$. The dimension of the space-time is assumed as $D = n + 2$ so that for $n = 2$ it reduces to ordinary 4-dimensional space-time geometry. We follow the treatment of Maharaj and Maartens [26] and write the energy momentum tensor of the anisotropic matter in the most general form filling the interior of the star in the form

$$T_{\alpha\beta} = (\rho + p) u_\alpha u_\beta - p g_{\alpha\beta} + \Pi_{\alpha\beta} , \tag{3}$$

where ρ and p denote the energy-density and isotropic pressure of the fluid, respectively and u_α is the 4-velocity of the fluid. If the energy-momentum tensor $T_{\alpha\beta}$ is equal to zero, it implies the absence of matter, which in turn means there is no energy density or pressure. Since energy density and pressure are functions

of the metric potentials, their absence suggests that there is no mass, leading to a scenario where the space-time curvature for the particular metric in question would be non-existent.

The anisotropic stress-tensor $\Pi_{\alpha\beta}$ has the form

$$\Pi_{\alpha\beta} = \sqrt{3}\, S\left[C_\alpha C_\beta - \frac{1}{3}\left(u_{\alpha\beta} - g_{\alpha\beta}\right)\right], \tag{4}$$

where $C^\alpha = \left(0, -e^{\mu}, 0, 0\right)$. For a spherically symmetric anisotropic distribution, $S(r)$ denotes the magnitude of the anisotropic stress. The non-vanishing components of the energy-momentum tensor are the following:

$$T_0^0 = \rho, \quad T_1^1 = -\left(p + \frac{2S}{\sqrt{3}}\right), \quad T_2^2 = T_3^3 = -\left(p - \frac{S}{\sqrt{3}}\right). \tag{5}$$

Consequently, radial and tangential pressures of the fluid can be obtained as

$$p_r = -T_1^1 = \left(p + \frac{2S}{\sqrt{3}}\right), \tag{6}$$

$$p_t = -T_2^2 = \left(p - \frac{2S}{\sqrt{3}}\right), \tag{7}$$

so that

$$S = \frac{p_r - p_t}{\sqrt{3}}. \tag{8}$$

Using the space-time metric (2) and energy-momentum tensor (3) of the distribution the Einstein field equations are subsequently obtained as

$$8\pi G_D \rho = \frac{n(n-1)\left(1 - e^{-2\mu}\right)}{2r^2} + \frac{n\mu' e^{-2\mu}}{r}, \tag{9}$$

$$8\pi G_D p_r = \frac{n\nu' e^{-2\mu}}{r} - \frac{n(n-1)\left(1 - e^{-2\mu}\right)}{2r^2}, \tag{10}$$

$$8\pi G_D p_t = e^{-2\mu}\left(\nu'' + \nu'^2 - \nu'\mu' + \frac{(n-1)(\nu' - \mu')}{r}\right) - \frac{(n-1)(n-2)\left(1 - e^{-2\mu}\right)}{2r^2}, \tag{11}$$

where, a prime ($'$) denotes differentiation with respect to the radial parameter r.

By defining the mass $m(r)$ within a radius r as

$$m(r) = \int_0^r \frac{2\pi^{(n+1)/2}}{\Gamma\left((n+1)/2\right)} u^n \rho(u)\, du, \tag{12}$$

we get an equivalent description of the system as

$$e^{-2\mu} = 1 - \frac{8\pi G_D\, \Gamma\left((n+1)/2\right) m(r)}{n r^{n-1} \pi^{3/2}}, \tag{13}$$

$$nr\,\nu'(r-2m)=8\pi G_D p_r r^3+n(n-1)m\,, \tag{14}$$

$$-\frac{4}{r}\left(8\pi G_D\sqrt{3}\,S\right)=\frac{4}{r}\left(8\pi G_D p_r\right)\left[\frac{n-2}{n}+\frac{\nu' r}{n}\right]$$
$$+\frac{4}{n}\left(8\pi G_D p_r'\right)+\frac{4\nu'}{r^2}(n-2)e^{-2\mu}-\frac{2}{r^3}(n-1)(n-2)\left(e^{-2\mu}-1\right). \tag{15}$$

The solution of field equations is discussed in the next section.

3. *Modified Finch and Skea model and solution*. We use the ansatz

$$e^{2\mu}=\left(1+\frac{r^2}{R^2}\right)^s, \tag{16}$$

where $s>0$ is a dimensionless parameter and R is the curvature parameter having the dimension of length. By introducing the parameter s, one can impose constraints on the radius to achieve the desired compactness M/R of the model. By appropriately setting the compactness parameter s for a given mass, it becomes feasible to tune and adjust the compactness of the system. Note that the ansatz (16) is a generalization of the Finch and Skea model which can be regained by setting $s=1$.

Using Eq. (16) in Eqs. (9) and (12) we have the following

$$8\pi G_D\,\rho=\frac{\left(n(n-1)/2r^2\right)\left(1+r^2/R^2\right)\left[\left(1+r^2/R^2\right)^s-1\right]+ns/R^2}{\left(1+r^2/R^2\right)^{s+1}}, \tag{17}$$

$$m(r)=\frac{nr^{n-1}\,\pi^{(n+1)/2}}{8\pi G_D\,\Gamma\left((n+1)/2\right)}\left[1-\left(1+\frac{r^2}{R^2}\right)^{-s}\right]. \tag{18}$$

To integrate Eq. (14), we use the prescription of Sharma and Ratanpal [27] by assuming the radial pressure in the form

$$8\pi G_D p_r=\frac{p_0\left(1-r^2/R^2\right)}{R^2\left(1+r^2/R^2\right)^{s+1}}, \tag{19}$$

which is a reasonable assumption since the radial pressure vanishes at $r=R$. Consequently, the curvature parameter R in our model turns out to be the boundary of the star.

Substituting Eq. (19) in Eq. (14) we have

$$\nu'=\frac{n-1}{2}\frac{\left[\left(1+r^2/R^2\right)^s-1\right]}{r}+\frac{p_0 r\left(1-r^2/R^2\right)}{nR^2\left(1+r^2/R^2\right)}, \tag{20}$$

and integrating, we get

$$e^{2\nu} = C\left(1+\frac{r^2}{R^2}\right)^{2p_0/n} \exp\left[-\frac{p_0 r^2}{nR^2} + (n-1)\int_0^r \left[\left(1+\frac{u^2}{R^2}\right)^s - 1\right]\frac{du}{u}\right], \tag{21}$$

where C is a constant of integration.

Finally, using Eq. (16), Eq. (19) and Eq. (15), the anisotropy is obtained as

$$\begin{aligned} 8\pi G_D \sqrt{3}\, S = &-\frac{r}{n}\left[\frac{n(n-2)}{2r^2}\left(1-A_3(r)\right)+\frac{2nsA_3(r)}{\left(r^2+R^2\right)}\right]A_2(r)+A_4(r)\left[\frac{n-2}{n}+\frac{r}{n}A_2(r)\right] \\ &+\frac{2r}{nR}A_1(r)+(n-2)A_4(r)+\frac{(n-1)(n-2)}{r^2}-\frac{A_3(r)}{4}\left[\frac{4(n-2)}{r}+\frac{2(n-1)(n-2)}{r^2}\right], \end{aligned} \tag{22}$$

where

$$A_1(r) = \frac{p_0 r^2\left[(s+2)-sr^2/R^2\right]}{R^4\left(1+r^2/R^2\right)^{s+2}}, \tag{23}$$

$$A_2(r) = \frac{(n-1)}{2r}\left[\left(1+r^2/R^2\right)^s - 1\right] + \frac{p_0 r\left[1-r^2/R^2\right]}{nR^2\left(1+r^2/R^2\right)}, \tag{24}$$

$$A_3(r) = \left(1+\frac{r^2}{R^2}\right)^{-s}, \tag{25}$$

$$A_4(r) = \frac{p_0\left(1-r^2/R^2\right)}{R^2\left(1+r^2/R^2\right)^{s+1}}. \tag{26}$$

Subsequently, the tangential pressure can be obtained from the relation

$$8\pi G_D p_t = 8\pi G_D p_r - 8\pi\sqrt{3S}\,. \tag{27}$$

Using the above relations, we also obtain $dp_r/d\rho$ and $dp_t/d\rho$.

Thus, our model has five unknown parameters namely, C, p_0, R, s and n which can be fixed by the appropriate boundary conditions as will be discussed in the following sections. To solve these equations, we must select two of the unknown model parameters independently (n, s). The remaining model parameters are then determined through boundary conditions. This approach allows us to solve Einstein's field equations and accurately model stellar configurations. Once the unknown model parameters are fully determined, we assess the physical plausibility of our model by evaluating whether the results align with known stellar properties. This validation process ensures that our model yields accurate and realistic results.

4. *Exterior space-time and matching conditions.* For spherically symmetric matter distributions, the vacuum solutions of Einstein's field equations are described by the Schwarzschild solution. This solution characterizes the space-time outside a non-rotating, spherically symmetric mass and is considered a vacuum solution because it applies in regions where the energy density is zero, i.e., outside the mass distribution. While modelling anisotropic compact stellar objects, the Schwarzschild vacuum solution is relevant only outside the star, where no matter is present. In the specific context of anisotropic compact stellar models, the vacuum solution would typically be considered outside the matter distribution, not within the star itself. To ensure physical consistency, the Schwarzschild exterior solution must match smoothly with the interior solution at the boundary of the stellar matter. The exterior region of the sphere is described by the Schwarzschild metric

$$ds_+^2 = -\left(1-\frac{2M_h}{r^{n-1}}\right)dt^2+\left(1-\frac{2M_h}{r^{n-1}}\right)^{-1}dr^2+r^2 d\Omega_n\,, \tag{28}$$

where M_h is related to the mass M as $M_h = 16\pi G_D M/n\Omega_n$. The matching conditions across the boundary surface $r=R$ to be fulfilled are

$$e^{2\nu(R)} = \left(1-\frac{2M_h}{r^{n-1}}\right), \tag{29}$$

$$e^{-2\mu(R)} = \left(1-\frac{2M_h}{r^{n-1}}\right), \tag{30}$$

where $m(R) = M_h$ is the total mass enclosed within the radius R.

The above boundary conditions yield

$$R^{n-1} = \frac{2^{s+1}M_h}{2^s-1}, \tag{31}$$

$$C = \exp\left[\frac{p_0}{n}-(n-1)\int_0^R\left[\left(1+\frac{r^2}{R^2}\right)^s-1\right]\frac{dr}{r}\right]2^{-(s+2p_0/n)}. \tag{32}$$

Eq. (31) clearly shows that the compactness of the stellar configuration M/R will depend on the parameters s and n. This contrasts with the earlier model developed by Sharma and Ratanpal [27], where s was set to 1, and thus did not account for this dependence.

5. *Physical conditions.* A physically acceptable stellar model must satisfy certain physical conditions

(i) The pressures and density should be positive, ρ, p_r, $p_t > 0$.

(ii) Radial pressure p_r should be zero at boundary $r=R$ i.e. $p_r\ (r=R)=0$.

(iii) The density and pressures should be maximum at the centre and

monotonically decreasing towards the boundary of the sphere, which requires the following relations:

$(d\rho/dr)_{r=0}=0$, $(dp_r/dr)_{r=0}=0$, $(dp_t/dr)_{r=0}=0$ and $(d^2\rho/dr^2)_{r=0}<0$, $(d^2p_r/dr^2)_{r=0}<0$, $(d^2p_t/dr^2)_{r=0}<0$ so that the density gradients and pressure gradients $d\rho/dr<0$, $dp_r/dr<0$, $dp_t/dr<0$ for $0<r\le R$.

(iv) The condition that the speed of the sound does not exceed light speed requires that, $0\le\sqrt{dp_r/d\rho}\le 1$, $0\le\sqrt{dp_t/d\rho}\le 1$.

(v) It must satisfy strong energy condition (SEC): $\rho+p_r+2p_t\ge 0$.

Also the trace energy condition (TEC), or $\rho-p_r-2p_t\ge 0$, should be positive throughout the star's interior, as proposed by Bondi [28] and Tello-Ortiz et al. [29].

To show that the developed model is regular, well-behaved and capable of describing realistic stars, we have considered the data of the pulsar 4U1820 - 30 whose mass and radius have recently been estimated to be $M=1.58M_\odot$ and $R=9.1$ km, respectively [30].

For stability, in general, the adiabatic index

$$\Gamma=\frac{\rho+p_r}{p_r}\frac{dp_r}{d\rho}, \tag{33}$$

should be greater than 4/3 according [31].

5.1. *Bound calculation*. In order to examine the unknown parameter p_0, we use boundary conditions.

(i) For $n=2$ and $s=1.1$

· The condition p_t $(r=R)>0$ if $p_0<1.28$ and for p_t $(r=0)>0$ if $p_0>0$.

· The expression $0<dp_r/d\rho<1$ $(r=R)$, if $0<p_0<3.5$ and $0<dp_r/d\rho<1$ $(r=0)$ for $0<p_0<1.86$.

· The expression $0<dp_t/d\rho<1$ $(r=R)$, if $0.43<p_0<5.1$ and $0<dp_t/d\rho<1$ $(r=0)$ for $0.17<p_0<1.41$.

· The expression of SEC $(r=R)>0$, if $0<p_0<3.53$ and SEC $(r=0)>0$, if $p_0>0$.

· The expression of TEC $(r=R)>0$, if $p_0>0$ and TEC $(r=0)>0$, if $0<p_0<1.104$. So for $n=2$ and $s=1.1$, our final bound is $0.43<p_0<1.1$. In this work, we choose $p_0=0.44$ for $n=2$ and $s=1.1$.

(ii) For $n=3$ and $s=1.1$

· The condition p_t $(r=R)>0$ if $p_0<5.8$ and for p_t $(r=0)>0$ if $p_0>0$.

· The expression $0<dp_r/d\rho<1$ $(r=R)$, if $0<p_0<7.05$ and $0<dp_r/d\rho<1$ $(r=0)$ for $0<p_0<3.36$.

· The expression $0<dp_t/d\rho<1$ $(r=R)$, if $1.08<p_0<6.9$ and $0<dp_t/d\rho<1$ $(r=0)$ for $0.60<p_0<3.49$.

· The expression of SEC $(r=R)>0$, if $0<p_0<13.4$ and SEC $(r=0)>0$,

if $p_0 > 0$.

· The expression of TEC $(r = R) > 0$, if $p_0 > 0$ and TEC $(r = 0) > 0$, if $0 < p_0 < 2.2$.

So for $n = 3$ and $s = 1.1$, our final bound is $1.08 < p_0 < 2.2$. In this paper, we choose $p_0 = 1.5$ for $n = 3$ and $s = 1.1$.

(iii) For $n = 4$ and $s = 1.1$

· The condition p_t $(r = R) > 0$ if $p_0 < 15$ and for p_t $(r = 0) > 0$ if $p_0 > 0$.

· The expression $0 < dp_r / d\rho < 1$ $(r = R)$, if $0 < p_0 < 11.7$ and $0 < dp_r / d\rho < 1$ $(r = 0)$ for $0 < p_0 < 5.23$.

· The expression $0 < dp_t / d\rho < 1$ $(r = R)$, if $2.05 < p_0 < 10.2$ and $0 < dp_t / d\rho < 1$ $(r = 0)$ for $1.3 < p_0 < 6.6$.

· The expression of SEC $(r = R) > 0$, if $0 < p_0 < 33.7$ and SEC $(r = 0) > 0$, if $p_0 > 0$.

· The expression of TEC $(r = R) > 0$, if $p_0 > 0$ and TEC $(r = 0) > 0$, if $0 < p_0 < 3.68$.

So for $n = 4$ and $s = 1.1$, our final bound is $2.05 < p_0 < 3.68$. In this paper, we choose $p_0 = 2.5$ for $n = 4$ and $s = 1.1$.

(iv) For $n = 5$ and $s = 1.1$

· The condition p_t $(r = R) > 0$ if $p_0 < 32$ and for p_t $(r = 0) > 0$ if $p_0 > 0$.

· The expression $0 < dp_r / d\rho < 1$ $(r = R)$, if $0 < p_0 < 17.7$ and $0 < dp_r / d\rho < 1$ $(r = 0)$ for $0 < p_0 < 7.4$.

· The expression $0 < dp_t / d\rho < 1$ $(r = R)$, if $3.3 < p_0 < 14.5$ and $0 < dp_t / d\rho < 1$ $(r = 0)$ for $2.3 < p_0 < 10.8$.

· The expression of SEC $(r = R) > 0$, if $0 < p_0 < 68.03$ and SEC $(r = 0) > 0$, if $p_0 > 0$.

· The expression of TEC $(r = R) > 0$, if $p_0 > 0$ and TEC $(r = 0) > 0$, if $0 < p_0 < 5.52$.

So for $n = 5$ and $s = 1.1$, our final bound is $3.3 < p_0 < 5.52$. In this paper, we choose $p_0 = 3.5$ for $n = 5$ and $s = 1.1$.

We show that our suggested model is physically valid using a range of parameters and multiple physical tests. We presented graphical representations to aid in clarity for the pulsar 4U 1820 - 30. The matter density, transverse, and radial pressure inside the star object should all be positive for a physically plausible model. The radial pressure ought to disappear at the fluid sphere's surface. Additionally, there should be a negative gradients of pressure and density throughout the radius. We examine the impact of energy density and pressures for the anisotropic distribution of matter with increasing the dimensions of space-time. The curve of energy densities and pressures with different space-time dimensions is displayed in Fig.1. These figures demonstrate that pressures and energy density are both positive, reaching their maximum at the centres of stellar objects and

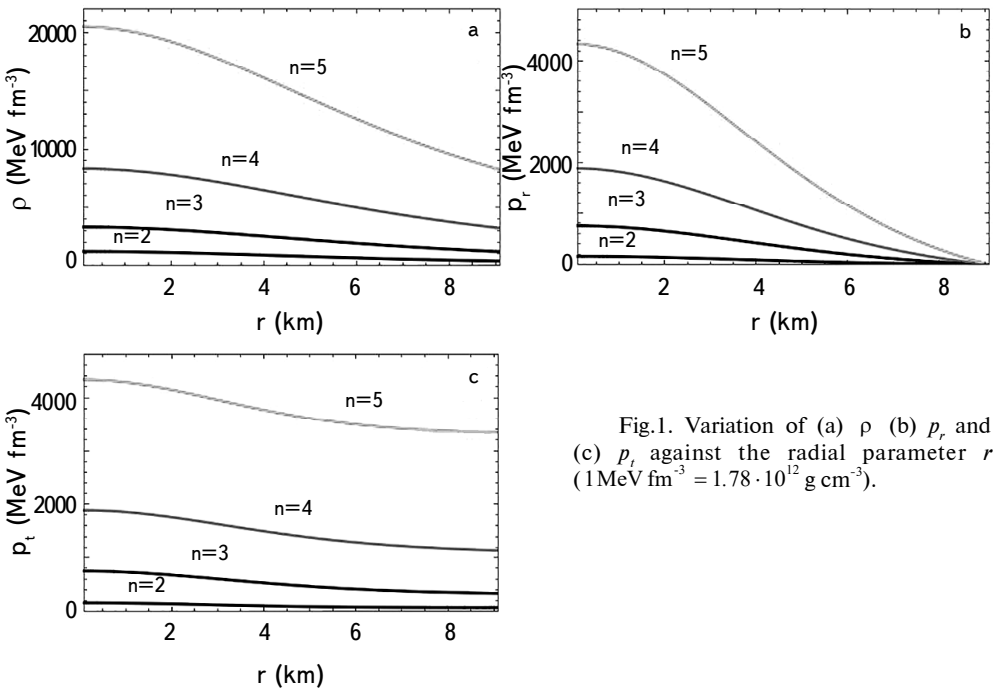

Fig.1. Variation of (a) ρ (b) p_r and (c) p_t against the radial parameter r ($1\,\mathrm{MeV\,fm^{-3}} = 1.78 \cdot 10^{12}\,\mathrm{g\,cm^{-3}}$).

monotonically declining towards their surfaces as needed. Whereas the radial pressure approaches zero at the star's border, ρ and p_t are both positive. In Fig.2 the profiles of density and pressure gradients are displayed. Plots demonstrate that these are all negative throughout the stellar interior, confirming the monotonically declining functions of ρ, p_r, and p_t. Here, we can observe that the energy density and pressure values increase as the dimensions increase and stay positive throughout the matter distribution. In contrast, it decreases as the radial coordinate r increases. To ensure the stability of the star, the model must adhere to the causality requirement. The radial and transverse sound velocities in our model, which are less than one with different dimensions as well, are represented by Fig.3. Understanding the nature of matter content in relativity requires that the model adheres to the strong energy requirement, which is $\rho + p_r + 2\,p_t \geq 0$. Fig.4 displays the model's energy state and indicates that the model satisfies the energy criteria because the graph is positive across the matter distribution. The trace energy condition is also shows at Fig.4. As such, our energy-momentum tensor behaves nicely.

5.2. *Stability criteria.*

5.2.1. *Adiabatic index.* The adiabatic index is described as follows and given by [32]:

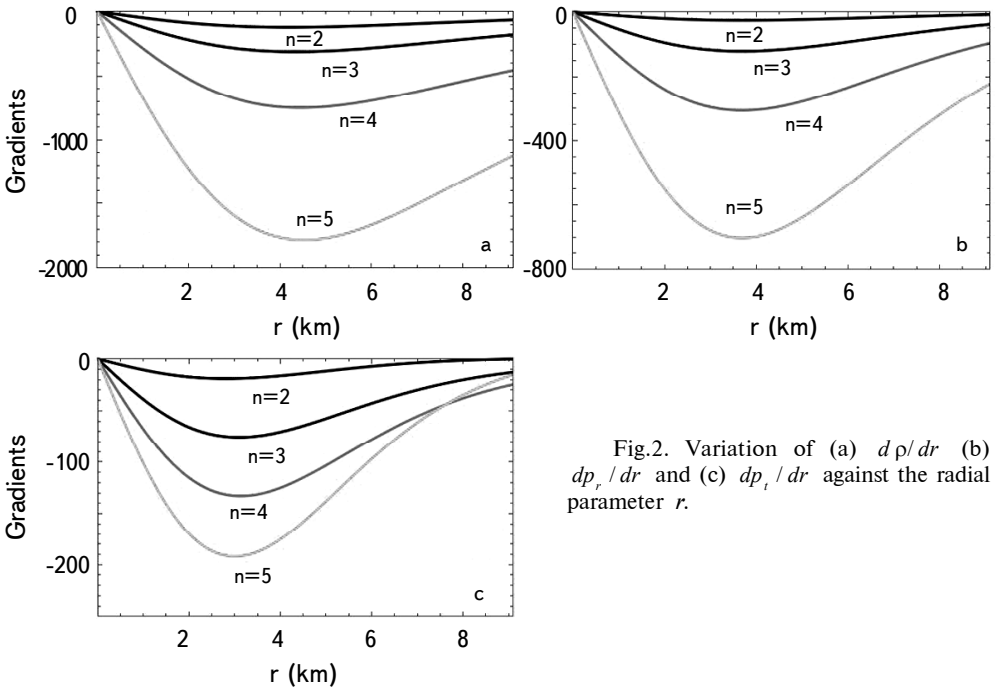

Fig.2. Variation of (a) $d\rho/dr$ (b) dp_r/dr and (c) dp_t/dr against the radial parameter r.

$$\Gamma = \frac{\rho + p_r}{p_r}\frac{dp_r}{d\rho}, \tag{34}$$

an anisotropic, relativistic star configuration's stability is correlated with its adiabatic index. Any star arrangement will remain stable if the adiabatic index is greater than 4/3. Fig.6a shows the variation of adiabatic index variation, which makes it evident that the configurations are stable and the model met the requirements for every dimension.

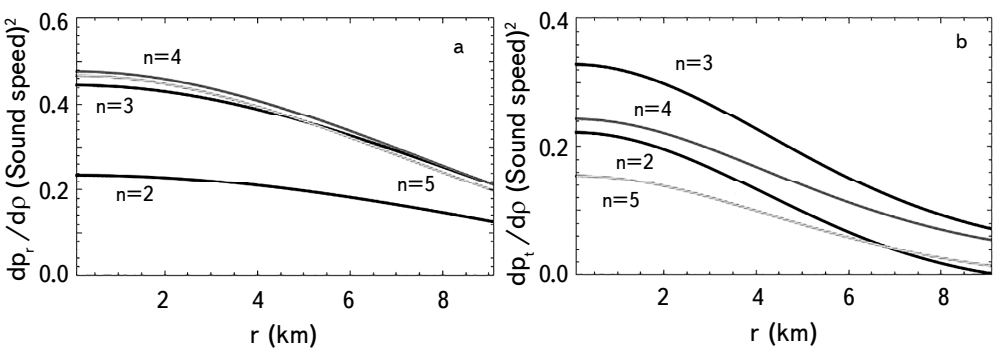

Fig.3. Variation of (a) $dp_r/d\rho$ and (b) $dp_t/d\rho$ against the radial parameter r.

5.2.2. *Cracking method*. Using Herrera's cracking idea [33], Abreu et al. [34] provides the following conditions for the model stability of an anisotropic matter distribution about the stability factor that if the model followers $-1 \leq v_{\perp}^2 - v_r^2 \leq 0$, then the model is a potentially stable model and model followers

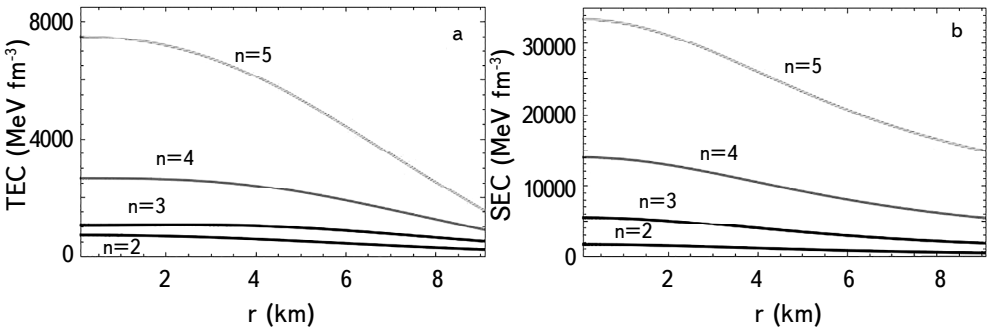

Fig.4. Variation of (a) $(\rho - p_r - 2p_t)$ and (b) $(\rho + p_r + 2p_t)$ against the radial parameter *r*.

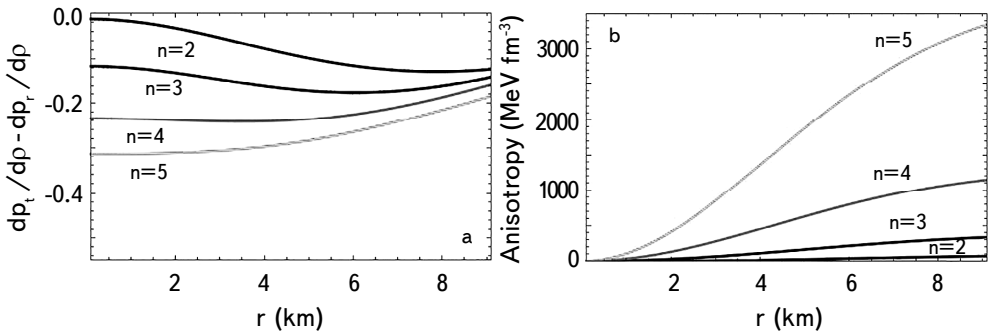

Fig.5. Variation of (a) $dp_t/d\rho - dp_r/d\rho$ and (b) Anisotropic parameter $S(r)$ against the radial parameter *r*.

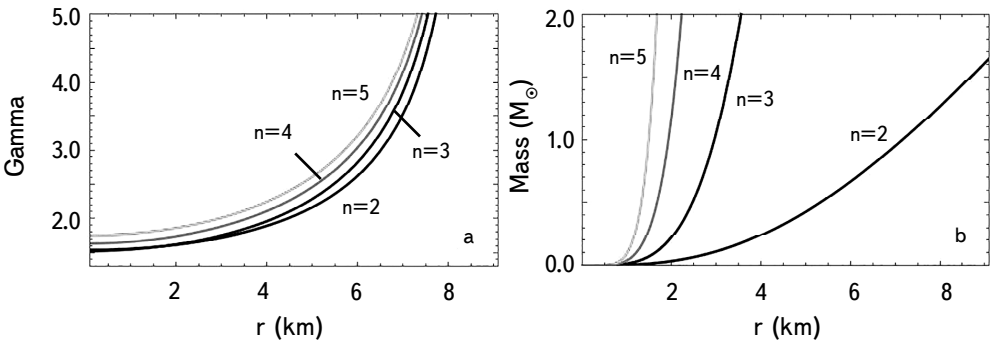

Fig.6. Variation of (a) Adiabatic index and (b) Mass against the radial parameter *r*.

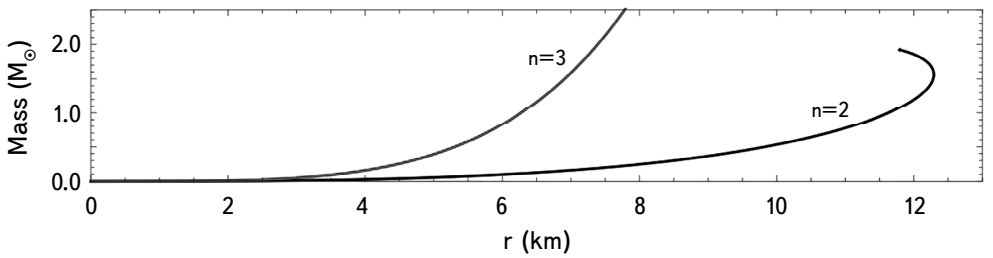

Fig.7. M - R plot.

$1 \le v_\perp^2 - v_r^2 \le 0$, then the model is potentially unstable. Given that the value of $-1 \le v_\perp^2 - v_r^2 \le 0$ in Fig.5a ranges between 0 and -1, we may conclude that this model has the potential stable in all dimensions.

6. *Discussion*. In this work, we have expanded the model originally proposed by Pandya and Thomas [9] by introducing a dimensionless parameter D (>0) into the modified Finch and Skea [1] ansatz and making the general assumption that the system is anisotropic. It is noteworthy that our modification of the Finch and Skea ansatz for the metric potential g_{rr} enables a fitting of the theoretically obtained compactness to the observed compactness of a given star. Additionally, an intriguing aspect of our approach is that, while it does not require a priori knowledge of the equation of state (EOS), we have successfully predicted the mass and radius of the pulsar. We have demonstrated that these assumptions can yield physically viable solutions suitable for modelling realistic stars. Specifically, our results indicate that by systematically adjusting the parameter s, the predicted masses and radii for the pulsar 4U 1820-30 align well with observational data. This suggests that our toy model is physically feasible for describing relativistic anisotropic compact stars, especially since we tested the pulsar 4U 1820 - 30 for $D = 4$ and higher dimensions, based on our findings. Fig.1 shows that all three physical quantities, ρ, p_r and p_t are of decreasing nature from the centre to the surface of the star 4U 1820 - 30 in four and higher dimensions. The radial variation of anisotropy is depicted in Fig.5b for $n = 2$ to $n = 5$, respectively. From this fig, it was clear that the magnitude of anisotropy is maximum at the star's surface and zero at the star's centre for all four and higher dimensions. Fig.6b shows that as the number of space-time dimensions (D) increases, the mass of a compact object also increases. It may be noted that for usual 4 - D ($n = 2$) the mass is $1.58\,M_\odot$ for radial parameter 9.8 km (radius). However, for the same star, the mass continues to increase as the number of dimensions rises. Thus, we infer that a compact object can accommodate more mass when observed in higher dimensions. We have also generated a mass-radius (M - R) plot for a fixed surface density of $4.7 \cdot 10^{14}$ g/cm^3. The (M - R) curve is plotted with the inclusion of the

dimensional factor (n). This plot allows us to predict how the maximum mass of a compact object will change depending on dimension factor. As observed in Fig.7, the maximum mass increases as the number of space-time dimensions rises. Notably, for the usual 4 - D space-time (where $n=2$), the maximum mass predicted by our model is approximately $2\,M_{\odot}$ and radius around 13 km, which is consistent with observational data. Therefore, by analyzing the (M - R) curve, the maximum allowed mass and radius of a compact star can be estimated across different space-time dimensions. In our present model by setting $n=2$, one can regain the modified Finch Skea model proposed earlier by Pandiya et al. [9]. Additionally, for $s=1$ the model reduces to the model mentioned in the work [35].

Acknowledgments. SD gratefully acknowledges support from the Inter-University Centre for Astronomy and Astrophysics (IUCAA), Pune, India, where part of this work was carried out under its Visiting Research Associateship Programme. BSR and AJ are thankful to IUCAA Pune for providing hospitality where part of this work was carried out.

[1] Department of Physics, Malaviya National Institute of Technology, Jaipur, 302017, India
[2] Department of Physics, Malda College, Malda 732101, India, e-mail: dasshyam321@gmail.com
[3] Department of Applied Mathematics, Faculty of Technology & Engineering, The Maharaja Sayajirao University of Baroda, Vadodara - 390 001, India

МОДИФИЦИРОВАННАЯ ЗВЕЗДНАЯ МОДЕЛЬ ФИНЧА И СКЕА В ВЫСШИХ ИЗМЕРЕНИЯХ

А.ДЖАНГИД[1], Ш.ДАС[2], Б.С.РАТАНПАЛ[3], К.К.ВЕНКАТАРАТНАМ[1]

В данном исследовании улучшена модель Пандьи и Томаса в рамках более высоких измерений и предположено, что система анизотропна в анзаце Финча и Скеа. Представленная модель исследует различные физические параметры в более высоких измерениях, включающих массу, плотность энергии, радиальное и поперечное давление и фактор анизотропии. Для анализа энергетических условий равновесия и устойчивости в различных измерениях используется графический метод. Кроме того, показано, что масса конкретного компактного объекта увеличивается с радиальными пара-

метрами по мере увеличения размерности пространства-времени. Кроме того, на графике масса-радиус (M-R) показано влияние размерностных факторов на максимальную массу и радиус, допустимые нашей моделью.

Ключевые слова: *модифицированный анзац Финча-Скеа: более высокие размерности: уравнения поля Эйнштейна: тензор Риччи*

REFERENCES

1. *M.R.Finch*, *J.E.Skea*, Classical and Quantum Gravity, **6**(4), 467, 1989.
2. *H.Duorah*, *R.Ray*, Classical and Quantum Gravity, **4**(6), 1691, 1987.
3. *M.Delgaty*, *K.Lake*, Computer Physics Communications, **115**(2-3), 395, 1998.
4. *M.Ruderman*, Ann. Rev. Astron. Astrophys., **10**(1), 427, 1972.
5. *V.Canuto*, Ann. Rev. Astron. Astrophys., **12**(1), 167, 1974.
6. *R.L.Bowers*, *E.Liang*, Astrophys. J., **188**, 657, 1974.
7. *S.Hansraj*, *S.Maharaj*, International Journal of Modern Physics D, **15**(08), 1311, 2006.
8. *B.Ratanpal*, *D.Pandya*, *R.Sharma et al.*, Astrophys. Space Sci., **362**(4), 82, 2017.
9. *D.Pandya*, *V.Thomas*, *R.Sharma*, Astrophys. Space Sci., **356**, 285, 2015.
10. *S.Maharaj*, *D.K.Matondo*, *P.M.Takisa*, International Journal of Modern Physics D, **26**(03), 1750014, 2017.
11. *A.Banerjee*, *F.Rahaman*, *K.Jotania et al.*, General Relativity and Gravitation, **45**(4), 717, 2013.
12. *P.Bhar*, *F.Rahaman*, *R.Biswas et al.*, Communications in Theoretical Physics, **62**(2), 221, 2014.
13. *T.Kaluza*, Zum unitätsproblem der physik. Sitzungsber. Preuss. Akad. Wiss. Berlin (Math. Phys.) **1921**(arXiv: 1803.08616), 966, 1921.
14. *O.Klein*, Theory of relativity, Z. Phys., **37**, 895, 1926.
15. *Q.Shafi*, *C.Wetterich*, Nuclear Physics B, **289**, 787, 1987.
16. *C.Wetterich*, Phys. Lett. B, **113**(5), 377, 1982.
17. *D.L.Wiltshire*, Phys. Rev. D, **38**(8), 2445, 1988.
18. *F.S.Accetta*, *M.Gleiser*, *R.Holman et al.*, Nuclear Phys. B, **276**(3-4), 501, 1986.
19. *B.Paul*, *S.Mukherjee*, Phys. Rev. D, **42**(8), 2595, 1990.
20. *A.Chodos*, *S.Detweiler*, Phys. Rev. D, **21**(8), 2167, 1980.
21. *A.Chodos*, *S.Detweiler*, General Relativity and Gravitation, **14**, 879, 1982.
22. *J.Garriga*, *T.Tanaka*, Phys. Rev. Lett., **84**(13), 2778, 2000.
23. *A.R.Liddle*, *R.Moorhouse*, *A.Henriques*, Classical and Quantum Gravity, **7**(6), 1009, 1990.

24. *B.C.Paul*, Classical and Quantum Gravity, **18**(14), 2637, 2001.
25. *S.A.Abel*, Phys. World, **12**(6), 21, 1999.
26. *S.Maharaj*, *R.Maartens*, General Relativity and Gravitation, **21**, 899, 1989.
27. *R.Sharma*, *B.Ratanpal*, International Journal of Modern Physics D, **22**(13), 1350074, 2013.
28. *S.H.Bondi*, Mon. Not. Roy. Astron. Soc., **302**(2), 337, 1999.
29. *F.Tello-Ortiz*, *S.Maurya*, *Y.Gomez-Leyton*, The European Physical Journal C, **80**(4), 324, 2020.
30. *T.Gangopadhyay*, *S.Ray*, *X.-D.Li et al.*, Mon. Not. Roy. Astron. Soc., **431**(4), 3216, 2013.
31. *H.Heintzmann*, *W.Hillebrandt*, Astron. Astrophys., **38**, 51, 1975.
32. *R.Chan*, *L.Herrera*, *N.Santos*, Mon. Not. Roy. Astron. Soc., **265**(3), 533, 1993.
33. *L.Herrera*, Phys. Lett. A, **165**(3), 206, 1992.
34. *H.Abreu*, *H.Hernández*, *L.A.Núnez*, Classical and Quantum Gravity, **24**(18), 4631, 2007.
35. *S.Dey*, *B.Paul*, Classical and Quantum Gravity, **37**(7), 075017, 2020.